Cancer Letters 466 (2019) 13–22

Contents lists available at ScienceDirect

Cancer Letters

journal homepage: www.elsevier.com/locate/canlet

Noninvasive imaging in cancer immunotherapy: The way to precision medicine

Yang Du[a,b,c,1], Yafei Qi[d,1], Zhengyu Jin[d,**], Jie Tian[a,b,d,e,f,*]

[a] CAS Key Laboratory of Molecular Imaging, The State Key Laboratory of Management and Control for Complex Systems, Institute of Automation, Beijing, 100190, China
[b] Beijing Key Laboratory of Molecular Imaging, Beijing, 100190, China
[c] University of Chinese Academy of Sciences, Beijing, 100080, China
[d] Department of Radiology, Peking Union Medical College Hospital, Chinese Academy of Medical Sciences & Peking Union Medical College, No. 1 Shuaifuyuan, Dongcheng District, Beijing, 100730, China
[e] Beijing Advanced Innovation Center for Big Data-Based Precision Medicine, School of Medicine, Beihang University, Beijing, 100191, China
[f] Engineering Research Center of Molecular and Neuro Imaging of Ministry of Education, School of Life Science and Technology, Xidian University, Xi'an, Shanxi, 710126, China

ARTICLE INFO

Keywords:
Precision medicine
Cancer
Immunotherapy
Molecular imaging
Immune checkpoint inhibitor

ABSTRACT

Molecular medicine requires a more precise treatment directed at molecular aberrations detected in tumors on an individual patient level. Immunotherapies empower the body's own immune system to confront tumor cells; however, their efficacy is often affected by tumor heterogeneity. Numerous noninvasive imaging techniques are available to monitor changes in tumor function reflecting therapeutic response, including immunotherapy, and to realize personalized response evaluation. For immunotherapy, strategies for using noninvasive imaging as a prognostic biomarker to identify patients who could benefit from targeted immunotherapy and predict early responders/nonresponders may ultimately lead to improved clinical management, individualized therapy regimens, and better prediction of patient outcomes. Herein, we summarize the recent progress in noninvasive imaging of immunotherapeutic targets such as immune cells, immune checkpoint inhibitors, immune vaccines, and T-cell therapy with chimeric antigen receptor, and review the clinical application of noninvasive imaging in immunotherapy. Finally, we describe the application of multimodal/multispectral imaging and radiomics, which may offer future direction for precision imaging in immunotherapy. With further progress of noninvasive imaging, guiding cancer immunotherapy into the era of precision medicine would be a promising option.

1. Introduction

From the emergence of imatinib, the first generation of targeted drugs against tumors, to the Precision Medicine Initiative, started by President Barack Obama in 2016, cancer research has entered the era of personalized identification and intervention [1]. Precision oncology calls for personalized interventions matched to suit patient requirements. Although conventional cancer treatments, including surgery, radiotherapy, and chemotherapy, are becoming more refined and systematic, novel cancer therapies that depend on signaling mechanisms and subcellular structure achieve clinical translation and obtain certain therapeutic effects [2]. Immunotherapy, using our own immune system to fight cancer, is considered as a revolutionary therapy relative to other systemic therapeutic strategies. The principles of immunotherapy involve enhancing immunotherapy to increase immune response and normalizing immunotherapy to restore a lost immune response. The enhancement strategies have generally been grouped in two: the first approach is to use effector cells/molecules of the immune system to directly attack tumor cells, which is called “passive” immunotherapy. The second approach is to enhance immune system activation through the modulation of endogenous regulatory and/or activating immune responses, which is called “active” immunotherapy. Normalization strategies aim to break the block or defects of the immune responses to reset a natural antitumor immune capacity [3,4].

* Corresponding author. CAS Key Laboratory of Molecular Imaging, The State Key Laboratory of Management and Control for Complex Systems, Institute of Automation, Beijing, 100190, China..
** Corresponding author.
E-mail addresses: jinzy@pumch.cn (Z. Jin), jie.tian@ia.ac.cn, tian@ieee.org (J. Tian).
URL: http://www.3dmed.net (J. Tian).
[1] These authors contributed equally to this paper.

https://doi.org/10.1016/j.canlet.2019.08.009
Received 17 January 2019; Received in revised form 13 July 2019; Accepted 20 August 2019

Abbreviations

CAR	chimeric antigen receptor
PD-1	programmed cell death protein 1
MSI-H	microsatellite instability-high
MMR-D	mismatch repair-deficient
TIL	tumor infiltrating lymphocyte
ICI	immune checkpoint inhibitor
TME	tumor microenvironment
T_{reg}	regulatory T lymphocyte
NK	natural killer
DCs	dendritic cells
CTL	cytotoxic T lymphocyte
TCR	T cell receptor
PET	positron emission tomography
MRI	magnetic resonance imaging
BLI	bioluminescence imaging
NIRF	near-infrared fluorescence
NIR-II	second near-infrared window
QDs	quantum dots
TAMs	tumor associated macrophages
mAb	monoclonal antibody
MDSCs	myeloid-derived suppressor cells
SPIONs	superparamagnetic iron oxide particles
CTLA-4	cytotoxic T-lymphocyte-associated protein 4
PD-L1	anti-programmed death ligand 1
CT	computed tomography
NSCLC	non-small cell lung cancer
PAI	photoacoustic imaging
irAE	immune-related adverse event

The success of immune checkpoint inhibitors (ICIs) and adoptive T-cell therapy with chimeric antigen receptor (CAR) are two revolutionary examples of immunotherapy that are changing the clinical management of cancer [5]. Pembrolizumab, an inhibitory antibody targeting the immune checkpoint receptor programmed cell death protein 1 (PD-1) approved by the Food and Drug Administration (FDA) in May 2017, is recommended for the treatment of unresectable or metastatic solid tumors with mismatch repair-deficient (dMMR) or microsatellite instability-high (MSI-H) [6]. In addition, Tisagenlecleucel, a cell-based gene therapy modified to a new gene that contains a CAR directing autologous T-cell immunotherapy approved by the FDA in May 2017, is recommended for the treatment of acute lymphoblastic leukemia [7]. However, the following three main challenges limit the further application of immunotherapy [8,9]. First, 50%–80% of cancer patients do not benefit from ICIs; second, traditional imaging methods only provide anatomic information, but do not define the concrete representation of response or progression, especially pseudo-progression owing to tumor infiltrating lymphocytes (TILs); and third, toxicities are a potential concern for the wide application of immunotherapy, which is associated with adverse events of the skin and spleen interacting with immune cells, antibodies, or cytokines. Hence, an accurate and reproducible imaging approach is urgently required to identify the population of patients most or least likely to respond to immunotherapy.

Molecular imaging, combined with disease-specific imaging probes,

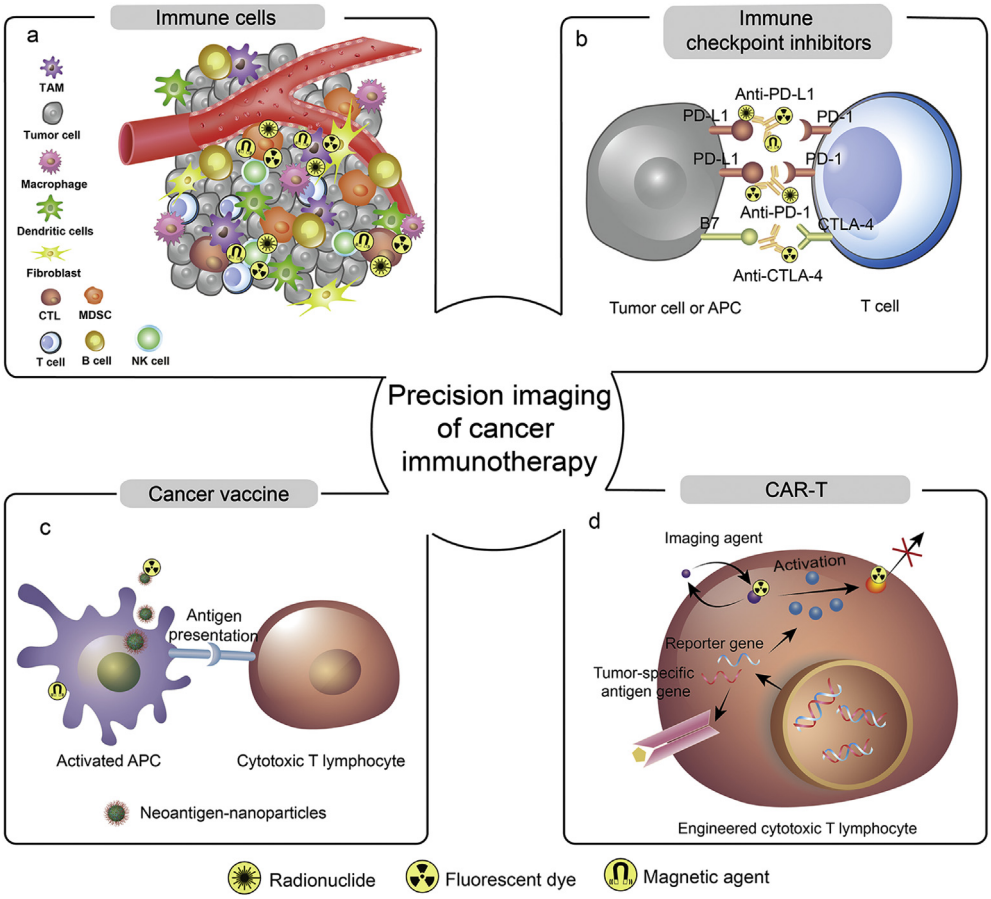

Fig. 1. Precision imaging of cancer immunotherapy targets. The non-invasive molecular imaging of immune cells, immune checkpoint inhibitors, tumor vaccines, and CAR-T.

can provide non-invasive, early and dynamic information about effects of immune cells or other cells in the tumor microenvironment (TME), as well as the target expression and the biodistribution of immunomodulatory drugs in the body, thereby allowing clinicians to predict which patients are most likely to benefit from immunotherapy [10]. In addition, combining immunotherapy with molecular imaging may realize the precision of cancer immunotherapy. Immunotherapies can be generally grouped into four major categories: (1) immune cell-based therapies, (2) ICIs, (3) tumor vaccines, and (4) CAR-T cell therapy. In this review, we focus on the advances in noninvasive molecular imaging of cancer immunotherapy, including immune cells, ICIs, tumor vaccines, and CAR-T (Fig. 1).

2. Imaging of immune cells and tumor microenvironment

Recently, more attention has been focused on immune cell-based therapies with the understanding of the complex interaction between immune cells and tumor cells in the TME [11]. In addition to tumor cells, TILs such as T cells, B cells, and natural killer (NK) cells, as well as macrophages and dendritic cells (DCs), are recruited to the TME and play important roles in regulating tumor growth and influencing anti-tumor therapeutic effects [12] (Fig. 2).

2.1. Imaging of immune T cells

Although some T cell subgroups such as regulatory T lymphocytes (Treg) inhibit tumor immunity, some T cell subgroups play a critical role in anti-tumor immunotherapy by activating cytotoxic T lymphocytes (CTLs). Thus far, the cancer immunotherapy response was primarily achieved through the T cell immune pathway, and the mechanisms are as follows. CTLs recognize an antigen–major histocompatibility complex (MHC) on a target cell through its T cell receptor (TCR). CTLs release the FAS ligand that engages FAS at the target cell membrane, which leads to apoptosis through FAS-associated death domain protein; next, CTLs release perforin and granzymes after recognizing cancer cells. Perforin opens a channel in the cancer cell membrane, allowing for granzymes to enter the cytoplasm of cancer cells, leading to their apoptosis [13].

Noninvasive imaging methods for tracking the homing and infiltrating T cells are mainly based on indirect cell labeling methods, including labeling with intact antibodies [14] or antibody fragments [15], cell metabolism-based labeling [16], and reporter gene-based labeling [17]. For example, Lehmann et al. developed a T-cell bispecific antibody (TCB)-carcinoembryonic antigen (CEA) by combining CD3 with CEA on tumor cells. They studied the pharmacokinetics of CEA TCB by using fluorescence imaging (FMI) in a mouse tumor model. The results showed that CEA TCB had the potential for the treatment of solid tumors [18]. OX40, also called CD134, is expressed in activated T cells. Additionally, Alam et al. developed and validated an anti-OX40 Ab-based PET imaging agent for specific and noninvasive detection of activated T cells with in situ administration of vaccine adjuvant -CpG oligonucleotide in A20 lymphoma bearing mice. The results showed that immuno-PET imaging integrating machine-learning approaches could be more accurate than anatomic imaging or a blood biomarker to predict a response to in situ cancer vaccines at earlier time points [19]. Direct cell labeling involves the isolation of immune cells *ex vivo* from the host and incubating them with the specific imaging tracer, and then transferring them back to the host for *in vivo* imaging. Stanton et al. utilized SPECT/PET-CT imaging to track the T cells labeled with Indium-111 homing to breast cancer and bone metastasis over 48 h [20].

2.2. Imaging of B cells

Studies relevant to the molecular imaging of B cells are rarely reported. Gonzalez et al. showed that CD40-positive B cells from luciferase- or GFP-transgenic mice homed to secondary lymphoid organs to activate CTL responses by acting as antigen presenting cells (APCs) in C57BL/6 mice [21]. This finding refined the potential of B cell-based cancer immunotherapy approaches.

2.3. Imaging of NK cells

Tumor cells are recognized and killed by NK cells without the need for antigen exposure or other prior treatment. The low expression of MHC-I and the high expression of inducible ligands on tumor cells can trigger NK cell activation, which directly induces tumor cell apoptosis

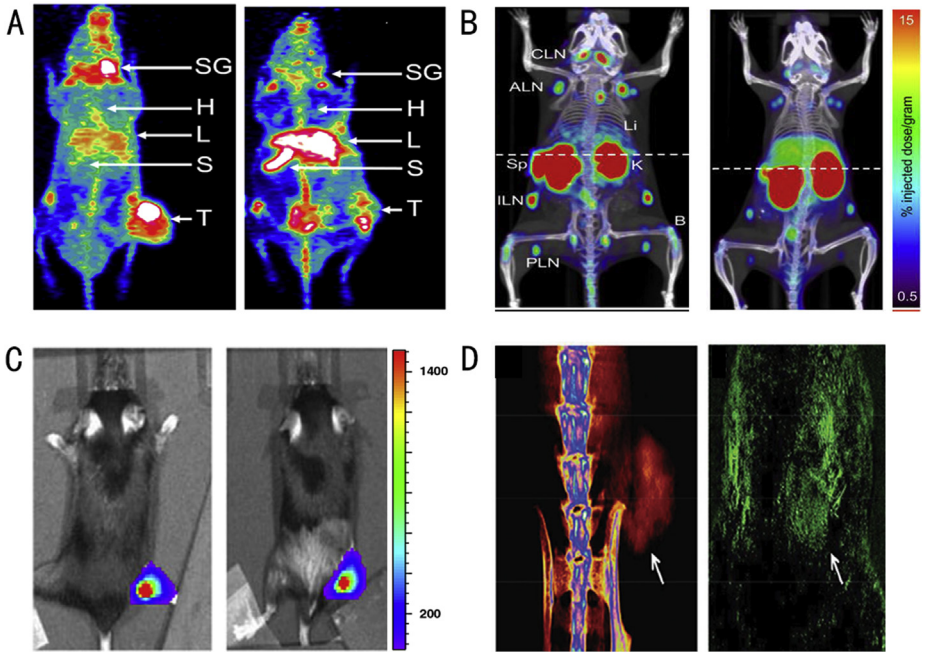

Fig. 2. Different strategies for molecular imaging of immune cells. (A) ^{89}Zr-Df-anti-PD-1 mAb targeting extracellular epitopes on the surface of T cells *in vivo* enables noninvasive PET imaging of T cells in A549 tumor-bearing human peripheral blood lymphocyte-severe combined immunodeficiency (PBL) and NSG mice. SG: salivary gland; H: heart; L: liver; S: Spleen; T: A549 tumor. Reproduced from Ref. [14]. (B) ^{89}Zr-malDFO-GK1.5 cys-diabody (anti-mouse CD4 antibody fragment) targeting extracellular epitopes at the surface of CD4$^+$ T cells enables *in vivo* noninvasive PET imaging of T cells in C57BL/6 with different doses of tracers. CLN: cervical lymphatic node (LN); ALN: axillary LN; Sp: spleen; Li: liver; K: kidney; ILN: inguinal LN; B: bone; PLN: popliteal LN. Reproduced from Ref. [15]. (C) Enhanced firefly luciferase (*Effluc*) gene was transduced into DC2.4 cells via retrovirus vectors. The *in vivo* bioluminescence imaging 1 and 3 d after administration of DC2.4/Effluc. Reproduced from Ref. [17]. (D) T cells were incubated with green fluorescent protein and gold nanoparticles *ex vivo*, and then the cells were injected into mice and tracked using CT and fluorescence imaging. The images show T cells accumulated at the tumor site. Reproduced from Ref. [42]. (For interpretation of the references to color in this figure legend, the reader is referred to the Web version of this article.)

via the perforin – granzymes pathway or expression of the FAS ligand, a death-receptor ligand [22]. Therefore, NK cell-based immunotherapies have remarkable potential for cancer treatment.

Molecular imaging strategies such as optical imaging (bioluminescence and fluorescence imaging), positron emission tomography (PET), and magnetic resonance imaging (MRI) were applied for *in vivo* NK cell tracking. NK-92MI cells were transfected with the luciferase gene, and bioluminescence imaging (BLI) was performed to dynamically track the bio-distribution of NK cells *in vivo*. The results showed that NK cells primarily accumulated in the lung and spleen at 1 h post-injection, and then gradually migrated to the tumor area 24 h post-injection [23]. Near-infrared fluorescence imaging (NIRF) is another safe, highly sensitive and non-invasive optical imaging method. ESNF13, an NIR fluorophore, was used to label NK cells. In non-tumor-bearing mice, NK cells localized primarily to the lungs immediately after injection, and then increased in the kidneys after 4 h. However, NK cells migrated to the tumor and metastasis area 4 h post-injection in MDA-MB-231 tumor-bearing NSG mice [24]. In another study, a fluorescence imaging in the second near-infrared window (NIR-II) was programmed to visualize the behaviors of two Ag2Se quantum dots (QDs) loaded with chemotherapy and labeling NK cells *in vivo*. Researchers first administered QDs (λEm = 1350 nm) loaded with stromal-cell-derived factor-1α (SDF-1α) and chemotherapy doxorubicin to the tumor site. Secondly, intravenously injected NK-92 cells labeled with another QD (λEm = 1050 nm) were localized to the tumor by the chemotaxis of SDF-1α. The approaches of chemotherapy and immunotherapy result in inhibition against a mouse model of human breast cancer and were evaluated by the imaging in NIR-II [25]. Intravital fluorescence microscopy was used to visualize the dynamic immune activity of NK cells. Deguine et al. utilized intravital fluorescence microscopy to monitor the short contact durations between GFP^+ endogenous NK cells and tumor cells. These results may offer new directions for the design of cancer immunotherapy [26]. PET imaging was used to trace NK cells directly labeled with radioisotopes or the biomolecules with radioisotopes targeting NK cells. Malviya et al. isolated and radiolabeled NK cells with ^{111}In-oxine to evaluate its biodistribution in the orthotopic human lung cancer mouse model. NK cells were found to accumulate mainly in the spleen and liver in SCID mice at 24 h post-injection. The mice bearing the orthotopic A549 human lung tumor showed higher lung uptake than the mice without lung tumors at 24 h post-injection [27]. In another study, the anti-CD56 monoclonal antibody radiolabeled with ^{99m}Tc was utilized to indirectly target NK cells. The study revealed that the ^{99m}Tc-anti-CD56 antibody physiologically accumulated in the liver and kidneys. ^{99m}Tc-anti-CD56 could be used to image NK cells accumulated in anaplastic thyroid cancer in CD1 nude mice 3 h post-injection [28]. Clinically applied heparin-protamine-ferumoxytol was also used to track NK cells during MRI. Results showed that labeled NK cells delivered via intraportal vein transcatheter or intravenous injection accumulated in the liver tissues after 0.5 h and migrated to liver tumor after 12 h [29].

2.4. Imaging of tumor-associated macrophages

A certain population of immuno-suppressive cells infiltrating into the TME to promote tumor growth is called tumor-associated macrophages (TAMs). Different phenotypic activation states of TAMs exist between tumoricidal M1 and pro-tumoral M2, depending on the interaction between TAMs and tumor cells [30]. TAMs tend to differentiate into the M2 phenotype by acquiring an immunosuppressive phenotype, and thus promote tumor growth and invasion [31].

Recently, many researchers studied the roles of TAMs in TME and traced their activity by using imaging. Arlauckas et al. used intravital fluorescence microscopy to trace a fluorescence-labeled anti-PD-1 monoclonal antibody (mAb). They showed that anti-PD-1 mAb effectively binds to $CD8^+$ T cells at early time-points, and is then captured by PD-1^- TAMs within minutes depending on the PD-1 mAb Fc. They further blocked the Fc domain *in vivo* before anti-PD-1 mAb administration, which prolonged the binding time to $CD8^+$ T cells and enhanced the immunotherapeutic effect [32]. Additionally, Aghighi et al. attempted to detect TAMs using ferumoxytol-enhanced MRI in lymphomas and bone sarcomas. They found that the T_2* signal on enhanced MR images significantly correlated with the number of TAMs [33]. Therefore, clinically applicable MRI may be effective at stratifing patients for immunotherapies and monitor therapeutic effects.

2.5. Imaging of myeloid-derived suppressor cells

Myeloid-derived suppressor cells (MDSCs) are another population of immuno-suppressed cells in the TME. MDSCs usually express CD11b and Gr-1 markers and are divided into polymorphonuclear MDSCs

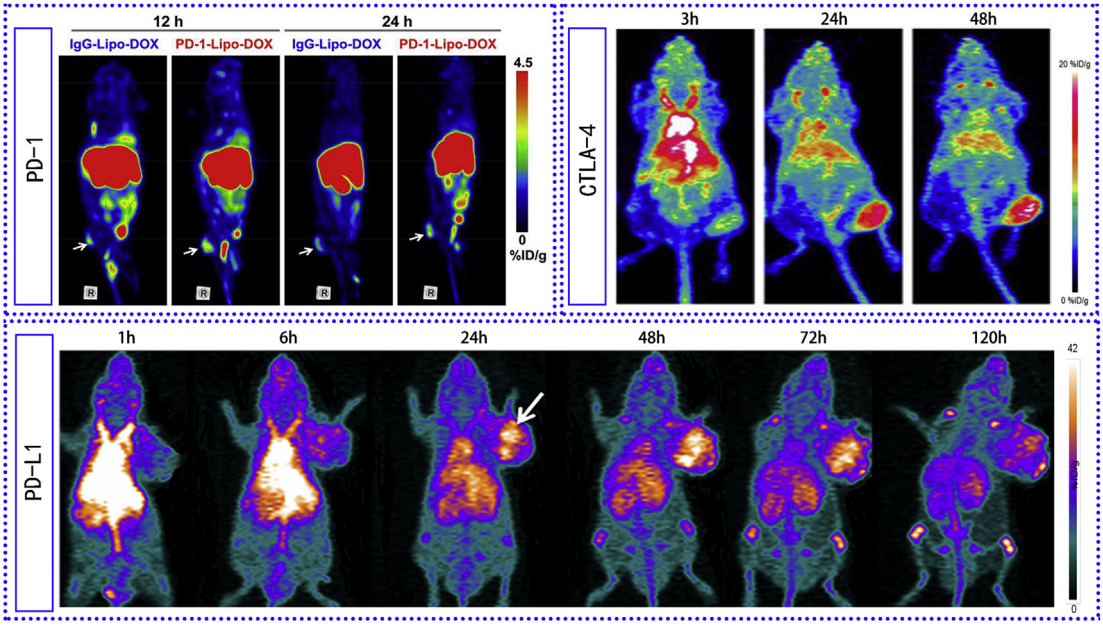

Fig. 3. Immuno-PET of ICIs. PET/CT imaging of PD-1-Liposome-DOX-^{64}Cu/IRDye800CW in mice bearing breast tumor, ^{89}Zr labeled anti-PD-L1 domain antibody in nude mice bearing LN229 xenografts and ^{64}Cu-DOTA-CTLA-4 in mice bearing non-small cell lung cancer. Reproduced from Refs. [51,57,63].

(PMN-MDSCs) and monocytic MDSCs (M-MDSCs) [34]. Specific negative regulatory functions have been described for MDSCs in immune responses: (1) immune suppression by inhibiting the function of T cells and NK cells as well as by inducing the expansion of Treg [35]; (2) increasing the resistance of patients to immune checkpoint inhibition [36]; and (3) promoting tumor invasion/metastasis and tumor angiogenesis [37].

The known characteristics of MDSCs allow molecular imaging to be used to trace the activity of MDSCs. Optical imaging was used to observe the recruitment and localization of fluorescently labeled MDSCs in breast tumor-bearing mice. The results revealed the influence of specific organs and TME on MDSC fate and function [38]. The MRI tracking of immune cells can be used to monitor the immunotherapeutic response and provide insight into the mechanism of activity. Tremblay et al. utilized superparamagnetic iron oxide particles (SPIONs) to label MDSCs and showed that the final tumor volumes were positively correlated with MDSC recruitment in immunotherapy [39]. In addition, Yu et al. developed MDSC membrane-coated SPIONs to achieve the function of immune evasion, active targeting, MRI, and photothermal therapy-induced tumor killing [40]. SPECT was also used to target MDSCs in colon cancer by using a Tc^{99m}-labeled anti-CD11b antibody, which facilitated the early detection of colon tumors in the inflammatory TME [41].

3. Imaging of ICIs

The success of ICI therapies have changed the treatment paradigm in oncology. The immune checkpoint pathway protects against self-tissue injury during immune responses; however, cancer cells can utilize it to escape an immune system attack [43]. ICIs such as anti-cytotoxic T-lymphocyte-associated protein-4 (CTLA-4) mAb, anti-PD-1 mAb, and anti-programmed death ligand-1 (PD-L1) mAb can exert anti-tumor immunity and induce durable cancer regression in pre-clinical trials [44](Fig. 3). Immune checkpoint blockade therapies are now approved by the FDA for the treatment of melanoma, renal cell carcinoma, non–small cell lung cancer (NSCLC), urothelial carcinoma, and other MSI-H or dMMR solid tumors [45].

3.1. Imaging of PD-1

PD-1, expressed on the surface of T cells and NK cells, acts as a negative regulator of cytotoxic immune cells. PD-L1, expressed on the surface of APCs or tumor cells, is an endogenous ligand that inhibits the activation of T-cells [46]. Despite its successful application in clinical trials, the therapeutic efficacy and responsiveness of anti-PD-1 agents vary remarkably among individual patients. Therefore, the development of new probes and tracers for identifying PD-1 expression is important to identify the population of patients that is likely to respond to immunotherapy [47].

Fluorescence optical imaging could be used to monitor probe biodistribution. Du et al. revealed the success of an IRDye800CW-labeled anti-PD-1 mAb probe for image-guided surgery in 4T1 breast tumors as well as in reducing tumor recurrences and metastases [48]. Recently, PET imaging was used to either evaluate the pharmacokinetics and biodistribution of anti-PD-1 Ab labeled with ^{89}zirconium (Zr) [49] or examine anti-PD-1 mAb labeled with ^{89}Zr or ^{64}Cu expression on TILs in mouse models [50]. PET imaging or fluorescence imaging has the advantages of bimodal imaging and could complement its own limitations. Du et al. showed that IRDye800CW and ^{64}Cu-labeled anti-PD-1 mAb-targeted Liposome-DOX had the potential for the diagnosis and treatment of breast tumors [51].

3.2. Imaging of PD-L1

PD-L1 is naturally expressed on the surface of several cells such as tumor cells, APCs, and T and B cells. PD-L1 blockade leads to enhanced activity of T cells and causes immune-mediated tumor inhibition [52]. The progress on three-dimensional optical imaging offers a quantitative method with cellular resolution. Lee et al. developed transparent tissue tomography to track the distribution of fluorescently labeled anti-PD-L1 Abs in whole tumors [53]. Computed tomography (CT) is applied for improving the treatment design by early identification of potential responders and nonresponders treated with the anti-PD-L1 antibody therapy. The anti-PD-L1 antibody-coated gold nanoparticles combined with CT imaging were developed as a powerful tool for predicting the therapeutic response [54]. Dual-modality imaging of NIRF and MRI were used by Du et al. to detect breast and colorectal tumors with theranostic cerasomes labeled with anti-PD-L1 antibodies [55] (Fig. 4A). Nuclear imaging plays a major role in detecting PD-L1 expression in tumors and the pharmacokinetics of an anti-PD-L1 Ab-conjugated agent with high sensitivity and functionality. The radiolabeled agents include ^{111}In-diethylenetriaminepentaacetic acid (DTPA)-anti-PD-L1 for SPECT imaging [56], ^{89}Zr-labeled anti-PD-L1 Ab domain antibody [57], ^{64}Cu-fibronectin type-3 domain-anti-PD-L1 Ab [58], and ^{18}F-labeled anti-PD-L1-Ab-binding molecule NOTA-$Z_{PD\text{-}L1\_1}$ for PET imaging [59].

3.3. Imaging of CTLA-4

The binding of CD28 and CD80/CD86 provides a co-stimulatory signal required for T cell activation. CTLA-4, an inhibitory receptor for CD80/CD86, is expressed on activated T lymphocytes. CD80/CD86 expressed on APCs can interact with CTLA-4 to inhibit the activity of T-cells via downregulation of CD28-mediated costimulatory signals [60]. The CTLA-4 blockade can effectively limit this interaction, thereby stimulating the production of active effector T cells. This strategy could possibly be exploited for the treatment of several cancers. PET has been used to visualize the CTLA-4 expression and biodistribution in Balb/c mice bearing CT26 tumors [61]. Recently, researchers have also identified CTLA-4 expression in NSCLC through PET imaging [62]. Ehlerding et al. utilized PET to investigate the accumulation of ^{64}Cu-DOTA-ipilimumab in NSCLC bearing mice [63].

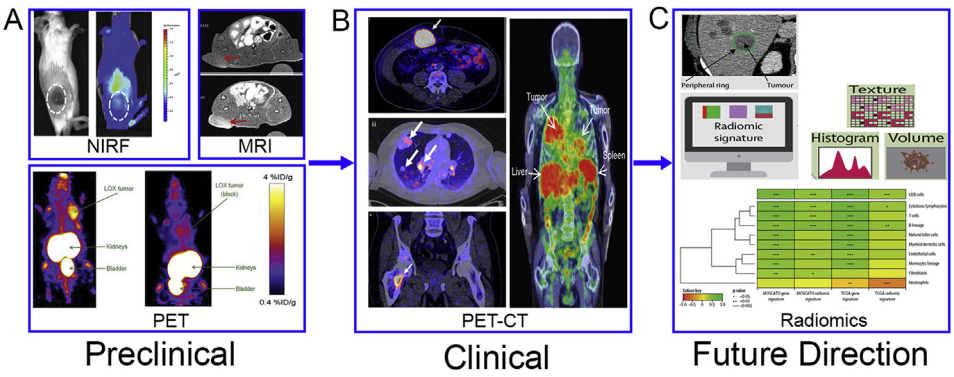

Fig. 4. Noninvasive imaging of ICIs in the preclinical and clinical phases and future directions. (A) *In vivo* IRDye800CW-fluorescence, Gd-MRI and ^{64}Cu-PET/CT imaging of PD-L1 in tumor-bearing mice. Reproduced from Refs. [55,59]. (B) PET/CT imaging with ^{89}Zr-atezolizumab biodistribution in tumor tissue and ^{89}Zr-labeled Nivolumab in the whole bodies of cancer patients. Reproduced from Refs. [108,109]. (C) A CT-based radiomics model was utilized to assess tumor-infiltrating $CD8^+$ T cells and predict clinical outcomes in patients treated with anti-PD-1 antibody or anti-PD-L1 antibody immunotherapy. Reproduced from Ref. [120].

4. Imaging of cancer vaccines

Tumor immune surveillance is characterized by the dynamic interaction between tumor cells and the immune system. Cancer immunity is characterized by specificity, which decreases off-target effects and increases immunological memory that controls tumor recurrence. These characteristics boost the development of cancer vaccines [64]. Cancer vaccines consist primarily of long peptide vaccines, viral vector vaccines, as well as RNA, DNA, engineered bacteria, and antigen-loaded DC vaccines. These vaccines have been used in both preclinical and clinical oncology studies [65] (Table 1).

MRI has been utilized to evaluate the differences in clearance efficacy between several different delivery systems of peptide-based cancer vaccines [81]. Verbeke et al. utilized fluorescence imaging with a lipophilic DiR fluorescent dye to visualize the biodistribution of nucleoside-modified mRNA vaccine [68]. ^{64}Cu-NOTA chelator was radiolabeled to DNA/RNA/peptide triple-co-delivery nanovaccines and imaging using PET technology to evaluate the delivery and immunostimulation of iDR-NCs on APCs in lymph nodes [78]. PET imaging with ^{124}I has been successfully used to monitor the therapeutic response of a virus vaccine (GLV-1h153) in pancreatic cancer xenografts [70]. Chen et al. engineered attenuated bacterial vector vaccine-magnetic nanoparticles to ablate tumors via photothermal therapy (PTT) under the guidance of MRI. *In vivo* MRI showed a 25% decrease T_2 signal intensity and a clear boundary at the tumor site [71].

4.1. Imaging of dendritic cell (DC) vaccines

The presentation and maturation of DC, a type of APC, is mandatory for the activation of T cells [82]. In tumor immunotherapy, DCs present tumor antigens to $CD8^+$ T cells via MHC-I. Mature DCs and pro-inflammatory cytokines provide costimulatory signals to $CD8^+$ T cells, which leads to anti-tumor responses by CTLs [83]. Therefore, DC vaccines are more efficient than other anticancer vaccines because they simultaneously integrate several signals to activate T cells.

Molecular imaging of DCs is important for evaluating their biodistribution [84], visualizing their activation [85], and determining the interactions between DCs and other immune cells [86], which may guide cancer immunotherapy in a precise manner [87]. The methods for labeling DCs can be divided into direct and indirect labeling. Crisci utilized SPIOs to label monocyte-derived DCs directly and MRI was utilized to monitor the migration and biodistribution of DCs in domestic pigs [88]. Liposome-coated gold nanocages loaded with adjuvant MPLA and specific anti-CD11c antibodies indirectly targeted DCs *in vivo* and stimulated the activation and maturation of DCs. These processes were monitored by fluorescence and photoacoustic imaging (PAI) [89]. The migration and biodistribution of DCs were also monitored by a radiotracer with nuclear imaging [90], quantum dots with near infrared imaging [73], and upconverting nanoparticles with upconversion luminescence imaging [91].

Molecular imaging allows for the precise visualization of the metabolism or fate of all therapeutic vaccines. It facilitates researchers to understand the activity and mechanism of vaccines, contributing to the formulation of key strategies in precision oncology for future vaccine development.

5. Imaging of CAR-T

CARs consist of an extracellular antigen-recognition domain and an intracellular signaling domain. They are transduced into T-cells via retroviral or lentiviral vectors [92]. The extracellular domains in CAR-T cells permit the recognition of a specific antigen, followed by the stimulation of T cell proliferation and cytokine secretion by the intracellular domains, leading to the attack of target cells [93]. CAR-T cell therapy has achieved progress in the treatment of $CD19^+$ hematologic malignancies,however, not in solid malignancies [7].

Therefore, molecular imaging techniques are urgently required to monitor the homing, distribution, and proliferation of CAR-T cells following adoptive transfer. Labeling methods of CAR-T cells include passive labeling [94] and reporter gene imaging [95]. PET with ^{89}Zr-Oxine [96], ^{111}Indium [97], and SPECT/CT with $^{99m}TcO_4$ [98] are used to directly label CAR-T cells and quantitatively evaluate their metabolism *in vivo*. Bajgain et al. used CAR-T cells modified with the tumor associated antigen to target metastatic breast cancer and BLI to track eGFP-Luc-CAR-T cells [99]. In the clinic, PET imaging with 9-[4-[^{18}F] fluoro-3-(hydroxymethyl) butyl] guanine has been performed for CAR-engineered CTLs transfected with the HSV1-tk reporter gene in nine recurrent glioma patients [100]. CAR-T therapy is an adoptive cell transfer therapy, which is a highly personalized therapy; therefore, molecular imaging may facilitate the precise application of CAR-T therapy to patients.

6. Clinical precision imaging of immunotherapy

With the successful application of immunotherapy in the clinic, response evaluation is essential for identifying patients who can benefit from immunotherapy, monitoring drug pharmacokinetics and pharmacodynamics, and predicting therapeutic outcomes in patients. For example, the radiologic pseudoprogression or the inflammatory response can be confused with conventional responses in cancer patients receiving immunotherapy [101–103]. Despite the existence of different tumor response criteria, including the response evaluation criteria in

Table 1
Noninvasive imaging of cancer vaccines.

Vaccine agent	Format	Modality	Reactivity	Stage	References
SPIO-DepoVax-R9F antigen	peptide	MRI	mice	Pre-clinic	[66]
RNA-lipoplexes encoding gp70	RNA	PET	mice	pre-clinic	[67]
DiR fluorescent dye- mRNA vaccine	RNA	FI	mice	pre-clinic	[68]
DNA encoding either tdTomato or luciferase	DNA	FI	mice	pre-clinic	[69]
^{124}I-GLV-1h153	virus	PET	mice	pre-clinic	[70]
Bacterial magnetic nanoparticle	Engineered attenuated bacterial vectors	MRI	mice	Pre-clinic	[71]
Antigen-loaded iron-labeled DC vaccine	DCs	MRI	mice	pre-clinic	[72]
SPIO/fluorophore EverGreen-GVAX	tumor cell	MRI/BLI	mice	Pre-clinic	[73]
NIR-QDs- DCs and tumor cell fused vaccine	fused cells	NIRF	mice	pre-clinic	[74]
DiR fluorescent dye -ovalbumin loaded pH/redox dual-sensitive micellar vaccine	Nano-vaccine	FI	mice	pre-clinic	[75]
OVA-zinc-doped iron oxide magnetic nanoparticles	Nano-vaccine	MRI	mice	pre-clinic	[76]
^{64}Cu-labeled NMEB-Adpgk	Nano-vaccine	PET	mice	pre-clinic	[77]
^{64}Cu-labeled DNA/RNA/peptide triple-co-delivery nanocarriers	Nano-vaccine	PET	mice	pre-clinic	[78]
GAA-derived HLA-A*0201-restricted peptides- TetA830 peptide-Seppic	peptide	MRI	patients	clinic	[79]
Tumor lysate/keyhole limpet hemocyanin-pulsed DC vaccination	DCs	PET	patients	clinic	[80]

Notes: SPIO: super-paramagnetic iron oxide; MRI: magnetic resonance imaging; PET: positron emission tomography; FI: fluorescence imaging; BLI: bioluminescence imaging; NIRF: near infrared fluorescence imaging; RNA: ribonucleic acid; DNA: deoxyribonucleic acid; DC: dendritic cell; QDs: quantum dots.

solid tumors (RECIST) 1.1, immune-related RECIST (irRECIST), iRECIST, and immune-related response criteria, no uniform criteria exist to evaluate responses after treatment [104]. Molecular imaging can advance the monitoring of changes in TME and immune status during the course of immunotherapy. In addition, molecular imaging contributes to the evaluation of immune-related adverse events caused by a non-specific response of immunotherapy.

PD-1 is expressed on the majority of TILs and PD-L1 is expressed on certain tumors. The metabolic parameters of PET imaging are correlated with the tissue expression of immune checkpoints in patients with NSCLC [105]. SUVmax and SUVmean are semi-quantitative parameters that have the potential to predict patients who may benefit from treatment with ICIs [106]. Toyokawa et al. analyzed CT features to identify PD-L1 expression before surgery in 394 patients with lung adenocarcinoma [107]. Direct labeling of ICIs has been verified in humans, providing insights into monitoring drug pharmacokinetics and treatment responses. Bensch et al. utilized a ^{89}Zr-labeled agent to assess the biodistribution of anti-PD-L1 antibodies in 22 patients with bladder cancer, NSCLC, or triple-negative breast cancer [108]. Niemeijer et al. successfully verified that PET imaging with ^{18}F-BMS-986192 and ^{89}Zr-Nivolumab (anti-PD-1 mAb) could be used to evaluate PD-1 and PD-L1 heterogeneous expression in 13 patients with advanced NSCLC prior to anti-PD-1 mAb therapy. Results also showed the relationship between tumor uptake of ^{18}F-BMS-986192 and ^{89}Zr-Nivolumab and response to anti-PD-1 mAb therapy [109] (Fig. 4B).

Immune-related adverse events (irAEs) caused by immunotherapies have been observed in different organs and systems. For example, thyroiditis, pneumonitis, and gastrointestinal irAEs are common. Therefore, early diagnosis and monitoring of irAEs is crucial for radiologists [110]. Studies have described radiological manifestations and clinicopathological features of common irAEs [111] and rare irAE such as nivolumab-related cholangitis [112] and sarcoid-like granulomatosis [113] in cancer patients with immunotherapy. Mekki et al. evaluated the rate of irAE detection by ^{18}F-FDG PET/CT, MRI, CT, ultrasonography, and X-rays. Results showed that medical imaging could detect 74% of irAEs in patients undergoing anti-PD1 Ab therapy [114].

Although the initial application of immunotherapy in the clinic has been successful, the development of more precise noninvasive imaging markers is needed to effectively personalize immunotherapy of patients with advanced cancers.

7. Future directions

The development of more precise methods to visualize the complex interactions between immune and tumor cells in the TME may be one of the promising future directions for immunotherapy. Multimodal imaging combines the advantages of two or more imaging modalities to facilitate earlier and more sensitive diagnosis. Multimodal imaging usually combines anatomical information with high spatial resolution and molecular biological information with high sensitivity [115]. Molecular imaging and theranostic nanoparticles can be designed to enable multimodal imaging via techniques such as NIRF, PET/SPECT, and MRI [55]. Moreover, multispectral imaging combined with the semi-quantitative immunofluorescence technique can simultaneously image the interactions of different populations of immune cells and tumor cells in the TME, providing a more precise evaluation of the immunotherapy [116]. For example, multispectral imaging studies have revealed that PD-1 is simultaneously expressed on CD4$^+$ T cells, CD8$^+$ T cells, Tregs and CD20$^+$ B cells in the TME of Merkel cell carcinoma [117]. In the future, multiplexed photoluminescent sensors based on organic materials maybe used to visualize the activities of different immune cells in the TME [118]. With progress in artificial intelligence and big data analysis, radiomics can be used to extract quantitative imaging features from clinical CT, PET, or MRI and offer a more comprehensive diagnostic approach, via the integration of genomics, molecular pathology, and clinical data, to uncover underlying cellular and molecular information [119]. As an illustration of the potential of this application, Sun et al. developed and validated a radiomic signature based on eight variables to assess the gene expression features of tumor-infiltrating CD8$^+$ T cells, immune phenotypes, and immunotherapy responses from contrast-enhanced CT images in four independent cohorts of patients with solid tumors [120] (Fig. 4C). In addition, Colen et al. utilized radiomics to predict patient risk for immunotherapy-induced pneumonitis, and irAEs [121]. Therefore, progress in both multi-modality imaging and radiomics may offer new directions for precision imaging in immunotherapy.

In conclusion, molecular imaging presents considerable potential for patient stratification, response assessment, and follow-up immunotherapy for precision oncology. However, specific considerations including safety evaluation and manufacturing process validation limit its further clinical translation for immunotherapy. Currently, molecular imaging has been proven to be feasible and effective for the assessment of immunotherapy in small patient samples. The forging of collaborative efforts between multi-disciplinary oncology teams has the potential to overcome the challenges associated with the use of these techniques and promote their clinical translation. Prospective multicenter clinical trials should be performed to validate observations and optimize assessment criteria. Only when these recommendations/proposals are adopted will molecular imaging fulfill its potential clinical application in precision oncology.

Conflicts of interest

There are no conflicts of interest to disclose.

Acknowledgements

The authors would like to thank Adjuvant Assitant Professor Dr. Karen M. von Deneen from the University of Fluorida for her English editing of this manuscript. This paper is supported by Ministry of Science and Technology of China under Grant No. 2017YFA0205; National Natural Science Foundation of China under Grant No. 81871514, 81227901, 81470083, 91859119; National Public Welfare Basic Scientific Research Program of Chinese Academy of Medical Sciences under Grant No. 2018PT32003, 2017PT32004.

References

[1] V. Prasad, T. Fojo, M. Brada, Precision oncology: origins, optimism, and potential, Lancet Oncol. 17 (2016) e81–e86.
[2] M. Gore, J. Larkin, Precision oncology: where next? Lancet Oncol. 16 (2015) 1593–1595.
[3] M.F. Sanmamed, L. Chen, A paradigm shift in cancer immunotherapy: from enhancement to normalization, Cell 175 (2018) 313–326.
[4] J. Galon, D. Bruni, Approaches to treat immune hot, altered and cold tumours with combination immunotherapies, Nat. Rev. Drug Discov. 18 (2019) 197–218.
[5] P. Sharma, S. Hu-Lieskovan, J.A. Wargo, A. Ribas, Primary, adaptive, and acquired resistance to cancer immunotherapy, Cell 168 (2017) 707–723.
[6] A. Ribas, J.D. Wolchok, Cancer immunotherapy using checkpoint blockade, Science 359 (2018) 1350–1355.
[7] C.H. June, R.S. O'Connor, O.U. Kawalekar, S. Ghassemi, M.C. Milone, CAR T cell immunotherapy for human cancer, Science 359 (2018) 1361–1365.
[8] D. Fukumura, J. Kloepper, Z. Amoozgar, D.G. Duda, R.K. Jain, Enhancing cancer immunotherapy using antiangiogenics: opportunities and challenges, Nat. Rev. Clin. Oncol. 15 (2018) 325–340.
[9] T.L. Whiteside, S. Demaria, M.E. Rodriguez-Ruiz, H.M. Zarour, I. Melero, Emerging opportunities and challenges in cancer immunotherapy, Clin. Cancer Res. 22 (2016) 1845–1855.
[10] R.A. Juergens, K.A. Zukotynski, A. Singnurkar, D.P. Snider, J.F. Valliant, K.Y. Gulenchyn, Imaging biomarkers in immunotherapy, Biomarkers Canc. 8 (2016) 1–13.
[11] M. Binnewies, E.W. Roberts, K. Kersten, V. Chan, D.F. Fearon, M. Merad, L.M. Coussens, D.I. Gabrilovich, S. Ostrand-Rosenberg, C.C. Hedrick, R.H. Vonderheide, M.J. Pittet, R.K. Jain, W. Zou, T.K. Howcroft, E.C. Woodhouse, R.A. Weinberg, M.F. Krummel, Understanding the tumor immune microenvironment (TIME) for effective therapy, Nat. Med. 24 (2018) 541–550.
[12] H. Wang, D.J. Mooney, Biomaterial-assisted targeted modulation of immune cells in cancer treatment, Nat. Mater. 17 (2018) 761–772.
[13] P. Golstein, G.M. Griffiths, An early history of T cell-mediated cytotoxicity, Nat.

Rev. Immunol. 18 (2018) 527–535.
[14] C.G. England, D. Jiang, E.B. Ehlerding, B.T. Rekoske, P.A. Ellison, R. Hernandez, T.E. Barnhart, D.G. McNeel, P. Huang, W. Cai, (89)Zr-labeled nivolumab for imaging of T-cell infiltration in a humanized murine model of lung cancer, Eur. J. Nucl. Med. Mol. Imaging 45 (2018) 110–120.
[15] A.C. Freise, K.A. Zettlitz, F.B. Salazar, X. Lu, R. Tavare, A.M. Wu, ImmunoPET imaging of murine CD4(+) T cells using anti-CD4 cys-diabody: effects of protein dose on T cell function and imaging, Mol. Imaging Biol. 19 (2017) 599–609.
[16] C. Klein, I. Waldhauer, V.G. Nicolini, A. Freimoser-Grundschober, T. Nayak, D.J. Vugts, C. Dunn, M. Bolijn, J. Benz, M. Stihle, S. Lang, M. Roemmele, T. Hofer, E. van Puijenbroek, D. Wittig, S. Moser, O. Ast, P. Brunker, I.H. Gorr, S. Neumann, M.C. de Vera Mudry, H. Hinton, F. Crameri, J. Saro, S. Evers, C. Gerdes, M. Bacac, G. van Dongen, E. Moessner, P. Umana, Cergutuzumab amunaleukin (CEA-IL2v), a CEA-targeted IL-2 variant-based immunocytokine for combination cancer immunotherapy: overcoming limitations of aldesleukin and conventional IL-2-based immunocytokines, OncoImmunology 6 (2017) e1277306.
[17] H. Lee, H.W. Lee, Y. La Lee, Y.H. Jeon, S.Y. Jeong, S.W. Lee, J. Lee, B.C. Ahn, Optimization of dendritic cell-mediated cytotoxic T-cell activation by tracking of dendritic cell migration using reporter gene imaging, Mol. Imaging Biol. 20 (2018) 398–406.
[18] S. Lehmann, R. Perera, H.P. Grimm, J. Sam, S. Colombetti, T. Fauti, L. Fahrni, T. Schaller, A. Freimoser-Grundschober, J. Zielonka, S. Stoma, M. Rudin, C. Klein, P. Umana, C. Gerdes, M. Bacac, In vivo fluorescence imaging of the activity of CEA TCB, a novel T-cell bispecific antibody, reveals highly specific tumor targeting and fast induction of T-cell-mediated tumor killing, Clin. Cancer Res. 22 (2016) 4417–4427.
[19] I.S. Alam, A.T. Mayer, I. Sagiv-Barfi, K. Wang, O. Vermesh, D.K. Czerwinski, E.M. Johnson, M.L. James, R. Levy, S.S. Gambhir, Imaging activated T cells predicts response to cancer vaccines, J. Clin. Investig. 128 (2018) 2569–2580.
[20] S.E. Stanton, J.F. Eary, E.A. Marzbani, D. Mankoff, L.G. Salazar, D. Higgins, J. Childs, J. Reichow, Y.S. Dang, M.L. Disis, Concurrent SPECT/PET-CT imaging as a method for tracking adoptively transferred T-cells in vivo, J Immunother Cancer 4 (2016) 27.
[21] N.K. Gonzalez, K. Wennhold, S. Balkow, E. Kondo, B. Bolck, T. Weber, M. Garcia-Marquez, S. Grabbe, W. Bloch, M. von Bergwelt-Baildon, A. Shimabukuro-Vornhagen, In vitro and in vivo imaging of initial B-T-cell interactions in the setting of B-cell based cancer immunotherapy, OncoImmunology 4 (2015) e1038684.
[22] L. Cifaldi, F. Locatelli, E. Marasco, L. Moretta, V. Pistoia, Boosting natural killer cell-based immunotherapy with anticancer drugs: a perspective, Trends Mol. Med. 23 (2017) 1156–1175.
[23] L. Zhu, X.J. Li, S. Kalimuthu, P. Gangadaran, H.W. Lee, J.M. Oh, S.H. Baek, S.Y. Jeong, S.W. Lee, J. Lee, B.C. Ahn, Natural killer cell (NK-92MI)-Based therapy for pulmonary metastasis of anaplastic thyroid cancer in a nude mouse model, Front. Immunol. 8 (2017) 816.
[24] T.N.T. Uong, K.H. Lee, S.J. Ahn, K.W. Kim, J.J. Min, H. Hyun, M.S. Yoon, Real-time tracking of ex vivo-expanded natural killer cells toward human triple-negative breast cancers, Front. Immunol. 9 (2018) 825.
[25] X. Hao, C. Li, Y. Zhang, H. Wang, G. Chen, M. Wang, Q. Wang, Programmable chemotherapy and immunotherapy against breast cancer guided by multiplexed fluorescence imaging in the second near-infrared window, Adv. Mater. 30 (2018) e1804437.
[26] J. Deguine, B. Breart, F. Lemaitre, J.P. Di Santo, P. Bousso, Intravital imaging reveals distinct dynamics for natural killer and CD8(+) T cells during tumor regression, Immunity 33 (2010) 632–644.
[27] G. Malviya, T. Nayak, C. Gerdes, R.A. Dierckx, A. Signore, E.F. de Vries, Isolation and (111)in-oxine labeling of murine NK cells for assessment of cell trafficking in orthotopic lung tumor model, Mol. Pharm. 13 (2016) 1329–1338.
[28] F. Galli, A.S. Rapisarda, H. Stabile, G. Malviya, I. Manni, E. Bonanno, G. Piaggio, A. Gismondi, A. Santoni, A. Signore, In vivo imaging of natural killer cell trafficking in tumors, J. Nucl. Med. 56 (2015) 1575–1580.
[29] K. Li, A.C. Gordon, L. Zheng, W. Li, Y. Guo, J. Sun, G. Zhang, G. Han, A.C. Larson, Z. Zhang, Clinically applicable magnetic-labeling of natural killer cells for MRI of transcatheter delivery to liver tumors: preclinical validation for clinical translation, Nanomedicine 10 (2015) 1761–1774.
[30] S. Zanganeh, R. Spitler, G. Hutter, J.Q. Ho, M. Pauliah, M. Mahmoudi, Tumor-associated macrophages, nanomedicine and imaging: the axis of success in the future of cancer immunotherapy, Immunotherapy 9 (2017) 819–835.
[31] Y. Komohara, Y. Fujiwara, K. Ohnishi, M. Takeya, Tumor-associated macrophages: potential therapeutic targets for anti-cancer therapy, Adv. Drug Deliv. Rev. 99 (2016) 180–185.
[32] S.P. Arlauckas, C.S. Garris, R.H. Kohler, M. Kitaoka, M.F. Cuccarese, K.S. Yang, M.A. Miller, J.C. Carlson, G.J. Freeman, R.M. Anthony, R. Weissleder, M.J. Pittet, In vivo imaging reveals a tumor-associated macrophage-mediated resistance pathway in anti-PD-1 therapy, Sci. Transl. Med. 9 (2017).
[33] M. Aghighi, A.J. Theruvath, A. Pareek, L.L. Pisani, R. Alford, A.M. Muehe, T.K. Sethi, S.J. Holdsworth, F.K. Hazard, D. Gratzinger, S. Luna-Fineman, R. Advani, S.L. Spunt, H.E. Daldrup-Link, Magnetic resonance imaging of tumor-associated macrophages: clinical translation, Clin. Cancer Res. 24 (2018) 4110–4118.
[34] F. Veglia, M. Perego, D. Gabrilovich, Myeloid-derived suppressor cells coming of age, Nat. Immunol. 19 (2018) 108–119.
[35] V. Kumar, S. Patel, E. Tcyganov, D.I. Gabrilovich, The nature of myeloid-derived suppressor cells in the tumor microenvironment, Trends Immunol. 37 (2016) 208–220.
[36] R. Weber, V. Fleming, X. Hu, V. Nagibin, C. Groth, P. Altevogt, J. Utikal, V. Umansky, Myeloid-derived suppressor cells hinder the anti-cancer activity of immune checkpoint inhibitors, Front. Immunol. 9 (2018) 1310.
[37] P. Qu, L.Z. Wang, P.C. Lin, Expansion and functions of myeloid-derived suppressor cells in the tumor microenvironment, Cancer Lett. 380 (2016) 253–256.
[38] J. Sceneay, C.M. Griessinger, S.H.L. Hoffmann, S.W. Wen, C.S.F. Wong, S. Krumeich, M. Kneilling, B.J. Pichler, A. Moller, Tracking the fate of adoptively transferred myeloid-derived suppressor cells in the primary breast tumor microenvironment, PLoS One 13 (2018) e0196040.
[39] M.L. Tremblay, C. Davis, C.V. Bowen, O. Stanley, C. Parsons, G. Weir, M. Karkada, M.M. Stanford, K.D. Brewer, Using MRI cell tracking to monitor immune cell recruitment in response to a peptide-based cancer vaccine, Magn. Reson. Med. 80 (2018) 304–316.
[40] G.T. Yu, L. Rao, H. Wu, L.L. Yang, L.L. Bu, W.W. Deng, L. Wu, X.L. Nan, W.F. Zhang, X.Z. Zhao, W. Liu, Z.J. Sun, Myeloid-derived suppressor cell membrane-coated magnetic nanoparticles for cancer theranostics by inducing macrophage polarization and synergizing immunogenic cell death, Adv. Funct. Mater. 28 (2018) 1801389.
[41] D. Cheng, W. Zou, X. Li, Y. Xiu, H. Tan, H. Shi, X. Yang, Preparation and evaluation of 99mTc-labeled anti-CD11b antibody targeting inflammatory microenvironment for colon cancer imaging, Chem. Biol. Drug Des. 85 (2015) 696–701.
[42] R. Meir, K. Shamalov, O. Betzer, M. Motiei, M. Horovitz-Fried, R. Yehuda, A. Popovtzer, R. Popovtzer, C.J. Cohen, Nanomedicine for cancer immunotherapy: tracking cancer-specific T-cells in vivo with gold nanoparticles and CT imaging, ACS Nano 9 (2015) 6363–6372.
[43] S.L. Topalian, C.G. Drake, D.M. Pardoll, Immune checkpoint blockade: a common denominator approach to cancer therapy, Cancer Cell 27 (2015) 450–461.
[44] S.A. Patel, A.J. Minn, Combination cancer therapy with immune checkpoint blockade: mechanisms and strategies, Immunity 48 (2018) 417–433.
[45] S.C. Wei, C.R. Duffy, J.P. Allison, Fundamental mechanisms of immune checkpoint blockade therapy, Cancer Discov. 8 (2018) 1069–1086.
[46] D.E. Dolan, S. Gupta, PD-1 pathway inhibitors: changing the landscape of cancer immunotherapy, Cancer Control 21 (2014) 231–237.
[47] F. Teng, X. Meng, L. Kong, J. Yu, Progress and challenges of predictive biomarkers of anti PD-1/PD-L1 immunotherapy: a systematic review, Cancer Lett. 414 (2018) 166–173.
[48] Y. Du, T. Sun, X. Liang, Y. Li, Z. Jin, H. Xue, Y. Wan, J. Tian, Improved resection and prolonged overall survival with PD-1-IRDye800CW fluorescence probe-guided surgery and PD-1 adjuvant immunotherapy in 4T1 mouse model, Int. J. Nanomed. 12 (2017) 8337–8351.
[49] C.G. England, E.B. Ehlerding, R. Hernandez, B.T. Rekoske, S.A. Graves, H. Sun, G. Liu, D.G. McNeel, T.E. Barnhart, W. Cai, Preclinical pharmacokinetics and biodistribution studies of 89Zr-labeled pembrolizumab, J. Nucl. Med. 58 (2017) 162–168.
[50] A. Natarajan, A.T. Mayer, R.E. Reeves, C.M. Nagamine, S.S. Gambhir, Development of novel ImmunoPET tracers to image human PD-1 checkpoint expression on tumor-infiltrating lymphocytes in a humanized mouse model, Mol. Imaging Biol. 19 (2017) 903–914.
[51] Y. Du, X. Liang, Y. Li, T. Sun, Z. Jin, H. Xue, J. Tian, Nuclear and fluorescent labeled PD-1-Liposome-DOX-(64)Cu/IRDye800CW allows improved breast tumor targeted imaging and therapy, Mol. Pharm. 14 (2017) 3978–3986.
[52] S.P. Patel, R. Kurzrock, PD-L1 expression as a predictive biomarker in cancer immunotherapy, Mol. Cancer Ther. 14 (2015) 847–856.
[53] S.S. Lee, V.P. Bindokas, S.J. Kron, Multiplex three-dimensional mapping of macromolecular drug distribution in the tumor microenvironment, Mol. Cancer Ther. 18 (2018) 213–226.
[54] R. Meir, K. Shamalov, T. Sadan, M. Motiei, G. Yaari, C.J. Cohen, R. Popovtzer, Fast image-guided stratification using anti-programmed death ligand 1 gold nanoparticles for cancer immunotherapy, ACS Nano 11 (2017) 11127–11134.
[55] Y. Du, X. Liang, Y. Li, T. Sun, H. Xue, Z. Jin, J. Tian, Liposomal nanohybrid cerasomes targeted to PD-L1 enable dual-modality imaging and improve antitumor treatments, Cancer Lett. 414 (2018) 230–238.
[56] J.R. Nedrow, A. Josefsson, S. Park, S. Ranka, S. Roy, G. Sgouros, Imaging of programmed cell death ligand 1: impact of protein concentration on distribution of anti-PD-L1 SPECT agents in an immunocompetent murine model of melanoma, J. Nucl. Med. 58 (2017) 1560–1566.
[57] D. Li, S. Cheng, S. Zou, D. Zhu, T. Zhu, P. Wang, X. Zhu, Immuno-pet imaging of (89)Zr labeled anti-PD-L1 domain antibody, Mol. Pharm. 15 (2018) 1674–1681.
[58] A. Natarajan, C.B. Patel, S. Ramakrishnan, P.S. Panesar, S.R. Long, S.S. Gambhir, A novel engineered small protein for positron emission tomography imaging of human programmed death ligand-1 : validation in mouse models and human cancer tissues, Clin. Cancer Res. 25 (2018) 1774–1785.
[59] D.E. Gonzalez Trotter, X. Meng, P. McQuade, D. Rubins, M. Klimas, Z. Zeng, B.M. Connolly, P.J. Miller, S.S. O'Malley, S.A. Lin, K.L. Getty, L. Fayadat-Dilman, L. Liang, E. Wahlberg, O. Widmark, C. Ekblad, F.Y. Frejd, E.D. Hostetler, J.L. Evelhoch, In vivo imaging of the programmed death ligand 1 by (18)F PET, J. Nucl. Med. 58 (2017) 1852–1857.
[60] E. Buchbinder, F.S. Hodi, Cytotoxic T lymphocyte antigen-4 and immune checkpoint blockade, J. Clin. Investig. 125 (2015) 3377–3383.
[61] K. Higashikawa, K. Yagi, K. Watanabe, S. Kamino, M. Ueda, M. Hiromura, S. Enomoto, 64Cu-DOTA-anti-CTLA-4 mAb enabled PET visualization of CTLA-4 on the T-cell infiltrating tumor tissues, PLoS One 9 (2014) e109866.
[62] L. Deng, B. Gyorffy, F. Na, B. Chen, J. Lan, J. Xue, L. Zhou, Y. Lu, Association of PDCD1 and CTLA-4 gene expression with clinicopathological factors and survival in non-small-cell lung cancer: results from a large and pooled microarray database, J. Thorac. Oncol. 10 (2015) 1020–1026.
[63] E.B. Ehlerding, C.G. England, R.L. Majewski, H.F. Valdovinos, D. Jiang, G. Liu,

D.G. McNeel, R.J. Nickles, W. Cai, ImmunoPET imaging of CTLA-4 expression in mouse models of non-small cell lung cancer, Mol. Pharm. 14 (2017) 1782–1789.
[64] K.K. Wong, W.A. Li, D.J. Mooney, G. Dranoff, Advances in therapeutic cancer vaccines, Adv. Immunol. 130 (2016) 191–249.
[65] U. Sahin, O. Tureci, Personalized vaccines for cancer immunotherapy, Science 359 (2018) 1355–1360.
[66] K.D. Brewer, K. Lake, N. Pelot, M.M. Stanford, D.R. DeBay, A. Penwell, G.M. Weir, M. Karkada, M. Mansour, C.V. Bowen, Clearance of depot vaccine SPIO-labeled antigen and substrate visualized using MRI, Vaccine 32 (2014) 6956–6962.
[67] S. Pektor, L. Hilscher, K.C. Walzer, I. Miederer, N. Bausbacher, C. Loquai, M. Schreckenberger, U. Sahin, M. Diken, M. Miederer, In vivo imaging of the immune response upon systemic RNA cancer vaccination by FDG-PET, EJNMMI Res. 8 (2018) 80.
[68] R. Verbeke, I. Lentacker, L. Wayteck, K. Breckpot, M. Van Bockstal, B. Descamps, C. Vanhove, S.C. De Smedt, H. Dewitte, Co-delivery of nucleoside-modified mRNA and TLR agonists for cancer immunotherapy: restoring the immunogenicity of immunosilent mRNA, J. Control. Release 266 (2017) 287–300.
[69] E. Kinnear, L.J. Caproni, J.S. Tregoning, A comparison of red fluorescent proteins to model DNA vaccine expression by whole animal in vivo imaging, PLoS One 10 (2015) e0130375.
[70] D. Haddad, P.B. Zanzonico, S. Carlin, C.H. Chen, N.G. Chen, Q. Zhang, Y.A. Yu, V. Longo, K. Mojica, R.J. Aguilar, A.A. Szalay, Y. Fong, A vaccinia virus encoding the human sodium iodide symporter facilitates long-term image monitoring of virotherapy and targeted radiotherapy of pancreatic cancer, J. Nucl. Med. 53 (2012) 1933–1942.
[71] C.F. Chen, S.H. Wang, L.L. Li, P.P. Wang, C.Y. Chen, Z.Y. Sun, T. Song, Bacterial magnetic nanoparticles for photothermal therapy of cancer under the guidance of MRI, Biomaterials 104 (2016) 352–360.
[72] Z. Zhang, W. Li, D. Procissi, K. Li, A.Y. Sheu, A.C. Gordon, Y. Guo, K. Khazaie, Y. Huan, G. Han, A.C. Larson, Antigen-loaded dendritic cell migration: MR imaging in a pancreatic carcinoma model, Radiology 274 (2015) 192–200.
[73] D.K. Kadayakkara, M.J. Korrer, J.W. Bulte, H.I. Levitsky, Paradoxical decrease in the capture and lymph node delivery of cancer vaccine antigen induced by a TLR4 agonist as visualized by dual-mode imaging, Cancer Res. 75 (2015) 51–61.
[74] C. Li, S. Liang, C. Zhang, Y. Liu, M. Yang, J. Zhang, X. Zhi, F. Pan, D. Cui, Allogenic dendritic cell and tumor cell fused vaccine for targeted imaging and enhanced immunotherapeutic efficacy of gastric cancer, Biomaterials 54 (2015) 177–187.
[75] D. Jiang, W. Mu, X. Pang, Y. Liu, N. Zhang, Y. Song, S. Garg, Cascade cytosol delivery of dual-sensitive micelle-tailored vaccine for enhancing cancer immunotherapy, ACS Appl. Mater. Interfaces 10 (2018) 37797–37811.
[76] A.I. Bocanegra Gondan, A. Ruiz-de-Angulo, A. Zabaleta, N. Gomez Blanco, B.M. Cobaleda-Siles, M.J. Garcia-Granda, D. Padro, J. Llop, B. Arnaiz, M. Gato, D. Escors, J.C. Mareque-Rivas, Effective cancer immunotherapy in mice by polyIC-imiquimod complexes and engineered magnetic nanoparticles, Biomaterials 170 (2018) 95–115.
[77] G. Zhu, G.M. Lynn, O. Jacobson, K. Chen, Y. Liu, H. Zhang, Y. Ma, F. Zhang, R. Tian, Q. Ni, S. Cheng, Z. Wang, N. Lu, B.C. Yung, Z. Wang, L. Lang, X. Fu, A. Jin, I.D. Weiss, H. Vishwasrao, G. Niu, H. Shroff, D.M. Klinman, R.A. Seder, X. Chen, Albumin/vaccine nanocomplexes that assemble in vivo for combination cancer immunotherapy, Nat. Commun. 8 (2017) 1954.
[78] G. Zhu, L. Mei, H.D. Vishwasrao, O. Jacobson, Z. Wang, Y. Liu, B.C. Yung, X. Fu, A. Jin, G. Niu, Q. Wang, F. Zhang, H. Shroff, X. Chen, Intertwining DNA-RNA nanocapsules loaded with tumor neoantigens as synergistic nanovaccines for cancer immunotherapy, Nat. Commun. 8 (2017) 1482.
[79] R. Ceschin, B.F. Kurland, S.R. Abberbock, B.M. Ellingson, H. Okada, R.I. Jakacki, I.F. Pollack, A. Panigrahy, Parametric response mapping of apparent diffusion coefficient as an imaging biomarker to distinguish pseudoprogression from true tumor progression in peptide-based vaccine therapy for pediatric diffuse intrinsic pontine glioma, AJNR Am J Neuroradiol 36 (2015) 2170–2176.
[80] M.S. Merchant, D. Bernstein, M. Amoako, K. Baird, T.A. Fleisher, M. Morre, S.M. Steinberg, M. Sabatino, D.F. Stroncek, A.M. Venkatasan, B.J. Wood, M. Wright, H. Zhang, C.L. Mackall, Adjuvant immunotherapy to improve outcome in high-risk pediatric sarcomas, Clin. Cancer Res. 22 (2016) 3182–3191.
[81] K.D. Brewer, G.M. Weir, I. Dude, C. Davis, C. Parsons, A. Penwell, R. Rajagopalan, L. Sammatur, C.V. Bowen, M.M. Stanford, Unique depot formed by an oil based vaccine facilitates active antigen uptake and provides effective tumour control, J. Biomed. Sci. 25 (2018) 7.
[82] R.L. Sabado, S. Balan, N. Bhardwaj, Dendritic cell-based immunotherapy, Cell Res. 27 (2017) 74–95.
[83] A.D. Garg, P.G. Coulie, B.J. Van den Eynde, P. Agostinis, Integrating next-generation dendritic cell vaccines into the current cancer immunotherapy landscape, Trends Immunol. 38 (2017) 577–593.
[84] Y. Xu, C. Wu, W. Zhu, C. Xia, D. Wang, H. Zhang, J. Wu, G. Lin, B. Wu, Q. Gong, B. Song, H. Ai, Superparamagnetic MRI probes for in vivo tracking of dendritic cell migration with a clinical 3 T scanner, Biomaterials 58 (2015) 63–71.
[85] D.R.J. Verboogen, N. Gonzalez Mancha, M. Ter Beest, G. van den Bogaart, Fluorescence Lifetime Imaging Microscopy reveals rerouting of SNARE trafficking driving dendritic cell activation, Elife 6 (2017) e23525.
[86] S. Van Lint, D. Renmans, K. Broos, L. Goethals, S. Maenhout, D. Benteyn, C. Goyvaerts, S. Du Four, K. Van der Jeught, L. Bialkowski, V. Flamand, C. Heirman, K. Thielemans, K. Breckpot, Intratumoral delivery of TriMix mRNA results in T-cell activation by cross-presenting dendritic cells, Cancer Immunol Res 4 (2016) 146–156.
[87] H. Jin, Y. Qian, Y. Dai, S. Qiao, C. Huang, L. Lu, Q. Luo, J. Chen, Z. Zhang, Magnetic enrichment of dendritic cell vaccine in lymph node with fluorescent-magnetic nanoparticles enhanced cancer immunotherapy, Theranostics 6 (2016) 2000–2014.
[88] E. Crisci, L. Fraile, R. Novellas, Y. Espada, R. Cabezon, J. Martinez, L. Cordoba, J. Barcena, D. Benitez-Ribas, M. Montoya, In vivo tracking and immunological properties of pulsed porcine monocyte-derived dendritic cells, Mol. Immunol. 63 (2015) 343–354.
[89] R. Liang, J. Xie, J. Li, K. Wang, L. Liu, Y. Gao, M. Hussain, G. Shen, J. Zhu, J. Tao, Liposomes-coated gold nanocages with antigens and adjuvants targeted delivery to dendritic cells for enhancing antitumor immune response, Biomaterials 149 (2017) 41–50.
[90] S.B. Lee, Y.J. Lee, S.J. Cho, S.K. Kim, S.W. Lee, J. Lee, D.K. Lim, Y.H. Jeon, Antigen-free radionuclide-embedded gold nanoparticles for dendritic cell maturation, tracking, and strong antitumor immunity, Adv. Healthc. Mater. 7 (2018) e1701369.
[91] J. Xiang, L. Xu, H. Gong, W. Zhu, C. Wang, J. Xu, L. Feng, L. Cheng, R. Peng, Z. Liu, Antigen-loaded upconversion nanoparticles for dendritic cell stimulation, tracking, and vaccination in dendritic cell-based immunotherapy, ACS Nano 9 (2015) 6401–6411.
[92] N. Emami-Shahri, S. Papa, Dynamic imaging for CAR-T-cell therapy, Biochem. Soc. Trans. 44 (2016) 386–390.
[93] H.J. Jackson, S. Rafiq, R.J. Brentjens, Driving CAR T-cells forward, Nat. Rev. Clin. Oncol. 13 (2016) 370–383.
[94] I. Serganova, E. Moroz, I. Cohen, M. Moroz, M. Mane, J. Zurita, L. Shenker, V. Ponomarev, R. Blasberg, Enhancement of PSMA-directed CAR adoptive immunotherapy by PD-1/PD-L1 blockade, Mol Ther Oncolytics 4 (2017) 41–54.
[95] S. Krebs, A. Ahad, L. Carter, J. Eyquem, C. Brand, M. Bell, V. Ponomarev, T. Reiner, C.F. Meares, S. Gottschalk, M. Sadelain, S.M. Larson, W.A. Weber, Antibody with infinite affinity for in vivo tracking of genetically engineered lymphocytes, J. Nucl. Med. 59 (2018) 1894–1900.
[96] M.R. Weist, R. Starr, B. Aguilar, J. Chea, J.K. Miles, E. Poku, E. Gerdts, X. Yang, S.J. Priceman, S.J. Forman, D. Colcher, C.E. Brown, J.E. Shively, PET of adoptively transferred chimeric antigen receptor T cells with (89)Zr-oxine, J. Nucl. Med. 59 (2018) 1531–1537.
[97] S.E. Stanton, J.F. Eary, E.A. Marzbani, D. Mankoff, L.G. Salazar, D. Higgins, J. Childs, J. Reichow, Y. Dang, M.L. Disis, Concurrent SPECT/PET-CT imaging as a method for tracking adoptively transferred T-cells in vivo, J Immunother Cancer 4 (2016) 27.
[98] N. Emami-Shahri, J. Foster, R. Kashani, P. Gazinska, C. Cook, J. Sosabowski, J. Maher, S. Papa, Clinically compliant spatial and temporal imaging of chimeric antigen receptor T-cells, Nat. Commun. 9 (2018) 1081.
[99] P. Bajgain, S. Tawinwung, L. D'Elia, S. Sukumaran, N. Watanabe, V. Hoyos, P. Lulla, M.K. Brenner, A.M. Leen, J.F. Vera, CAR T cell therapy for breast cancer: harnessing the tumor milieu to drive T cell activation, J Immunother Cancer 6 (2018) 34.
[100] K.V. Keu, T.H. Witney, S. Yaghoubi, J. Rosenberg, A. Kurien, R. Magnusson, J. Williams, F. Habte, J.R. Wagner, S. Forman, C. Brown, M. Allen-Auerbach, J. Czernin, W. Tang, M.C. Jensen, B. Badie, S.S. Gambhir, Reporter gene imaging of targeted T cell immunotherapy in recurrent glioma, Sci. Transl. Med. 9 (2017) eaag2196.
[101] S.I. Katz, M. Hammer, S.J. Bagley, C. Aggarwal, J.M. Bauml, J.C. Thompson, A.C. Nachiappan, C.B. Simone 2nd, C.J. Langer, Radiologic pseudoprogression during anti-PD-1 therapy for advanced non-small cell lung cancer, J. Thorac. Oncol. 13 (2018) 978–986.
[102] S. Ranjan, M. Quezado, N. Garren, L. Boris, C. Siegel, O. Lopes Abath Neto, B.J. Theeler, D.M. Park, E. Nduom, K.A. Zaghloul, M.R. Gilbert, J. Wu, Clinical decision making in the era of immunotherapy for high grade-glioma: report of four cases, BMC Canc. 18 (2018) 239.
[103] K. Ito, R. Teng, H. Schoder, J.L. Humm, A. Ni, L. Michaud, R. Nakajima, R. Yamashita, J.D. Wolchok, W.A. Weber, F-18 FDG PET/CT for monitoring of ipilimumab therapy in patients with metastatic melanoma, J. Nucl. Med. 60 (2018) 335–341.
[104] M. Tazdait, L. Mezquita, J. Lahmar, R. Ferrara, F. Bidault, S. Ammari, C. Balleyguier, D. Planchard, A. Gazzah, J.C. Soria, A. Marabelle, B. Besse, C. Caramella, Patterns of responses in metastatic NSCLC during PD-1 or PDL-1 inhibitor therapy: comparison of RECIST 1.1, irRECIST and iRECIST criteria, Eur. J. Cancer 88 (2018) 38–47.
[105] K. Takada, G. Toyokawa, T. Okamoto, S. Baba, Y. Kozuma, T. Matsubara, N. Haratake, T. Akamine, S. Takamori, M. Katsura, F. Shoji, H. Honda, Y. Oda, Y. Maehara, Metabolic characteristics of programmed cell death-ligand 1-expressing lung cancer on (18) F-fluorodeoxyglucose positron emission tomography/computed tomography, Cancer Med 6 (2017) 2552–2561.
[106] E. Lopci, L. Toschi, F. Grizzi, D. Rahal, L. Olivari, G.F. Castino, S. Marchetti, N. Cortese, D. Qehajaj, D. Pistillo, M. Alloisio, M. Roncalli, P. Allavena, A. Santoro, F. Marchesi, A. Chiti, Correlation of metabolic information on FDG-PET with tissue expression of immune markers in patients with non-small cell lung cancer (NSCLC) who are candidates for upfront surgery, Eur. J. Nucl. Med. Mol. Imaging 43 (2016) 1954–1961.
[107] G. Toyokawa, K. Takada, T. Okamoto, M. Shimokawa, Y. Kozuma, T. Matsubara, N. Haratake, S. Takamori, T. Akamine, M. Katsura, F. Shoji, Y. Oda, Y. Maehara, Computed tomography features of lung adenocarcinomas with programmed death ligand 1 expression, Clin. Lung Cancer 18 (2017) e375–e383.
[108] F. Bensch, E.L. van der Veen, M.N. Lub-de Hooge, A. Jorritsma-Smit, R. Boellaard, I.C. Kok, S.F. Oosting, C.P. Schroder, T.J.N. Hiltermann, A.J. van der Wekken, H.J.M. Groen, T.C. Kwee, S.G. Elias, J.A. Gietema, S.S. Bohorquez, A. de Crespigny, S.P. Williams, C. Mancao, A.H. Brouwers, B.M. Fine, E.G.E. de Vries, (89)Zr-atezolizumab imaging as a non-invasive approach to assess clinical response to PD-L1 blockade in cancer, Nat. Med. 24 (2018) 1852–1858.

[109] A.N. Niemeijer, D. Leung, M.C. Huisman, I. Bahce, O.S. Hoekstra, G. van Dongen, R. Boellaard, S. Du, W. Hayes, R. Smith, A.D. Windhorst, N.H. Hendrikse, A. Poot, D.J. Vugts, E. Thunnissen, P. Morin, D. Lipovsek, D.J. Donnelly, S.J. Bonacorsi, L.M. Velasquez, T.D. de Gruijl, E.F. Smit, A.J. de Langen, Whole body PD-1 and PD-L1 positron emission tomography in patients with non-small-cell lung cancer, Nat. Commun. 9 (2018) 4664.

[110] M. Nishino, H. Hatabu, F.S. Hodi, Imaging of cancer immunotherapy: current approaches and future directions, Radiology 290 (2019) 9–22.

[111] P. Sidhu, A.M. Menzies, G. Long, M. Carlino, S. Lorens, R. Kapoor, Radiological manifestations of immune-related adverse effects observed in patients with melanoma undergoing immunotherapy, J Med Imaging Radiat Oncol 61 (2017) 759–766.

[112] H. Kawakami, J. Tanizaki, K. Tanaka, K. Haratani, H. Hayashi, M. Takeda, K. Kamata, M. Takenaka, M. Kimura, T. Chikugo, T. Sato, M. Kudo, A. Ito, K. Nakagawa, Imaging and clinicopathological features of nivolumab-related cholangitis in patients with non-small cell lung cancer, Investig. New Drugs 35 (2017) 529–536.

[113] M. Nishino, L.M. Sholl, M.M. Awad, H. Hatabu, P. Armand, F.S. Hodi, Sarcoid-like granulomatosis of the lung related to immune-checkpoint inhibitors: distinct clinical and imaging features of a unique immune-related adverse event, Cancer Immunol Res 6 (2018) 630–635.

[114] A. Mekki, L. Dercle, P. Lichtenstein, A. Marabelle, J.M. Michot, O. Lambotte, J. Le Pavec, E. De Martin, C. Balleyguier, S. Champiat, S. Ammari, Detection of immune-related adverse events by medical imaging in patients treated with anti-programmed cell death 1, Eur. J. Cancer 96 (2018) 91–104.

[115] S.Y. Lee, S.I. Jeon, S. Jung, I.J. Chung, C.H. Ahn, Targeted multimodal imaging modalities, Adv. Drug Deliv. Rev. 76 (2014) 60–78.

[116] A. Mezheyeuski, C.H. Bergsland, M. Backman, D. Djureinovic, T. Sjoblom, J. Bruun, P. Micke, Multispectral imaging for quantitative and compartment-specific immune infiltrates reveals distinct immune profiles that classify lung cancer patients, J. Pathol. 244 (2018) 421–431.

[117] N.A. Giraldo, P. Nguyen, E.L. Engle, G.J. Kaunitz, T.R. Cottrell, S. Berry, B. Green, A. Soni, J.D. Cuda, J.E. Stein, J.C. Sunshine, F. Succaria, H. Xu, A. Ogurtsova, L. Danilova, C.D. Church, N.J. Miller, S. Fling, L. Lundgren, N. Ramchurren, J.H. Yearley, E.J. Lipson, M. Cheever, R.A. Anders, P.T. Nghiem, S.L. Topalian, J.M. Taube, Multidimensional, quantitative assessment of PD-1/PD-L1 expression in patients with Merkel cell carcinoma and association with response to pembrolizumab, J Immunother Cancer 6 (2018) 99.

[118] X.P. He, X.L. Hu, T.D. James, J. Yoon, H. Tian, Multiplexed photoluminescent sensors: towards improved disease diagnostics, Chem. Soc. Rev. 46 (2017) 6687–6696.

[119] P. Lambin, R.T.H. Leijenaar, T.M. Deist, J. Peerlings, E.E.C. de Jong, J. van Timmeren, S. Sanduleanu, R. Larue, A.J.G. Even, A. Jochems, Y. van Wijk, H. Woodruff, J. van Soest, T. Lustberg, E. Roelofs, W. van Elmpt, A. Dekker, F.M. Mottaghy, J.E. Wildberger, S. Walsh, Radiomics: the bridge between medical imaging and personalized medicine, Nat. Rev. Clin. Oncol. 14 (2017) 749–762.

[120] R. Sun, E.J. Limkin, M. Vakalopoulou, L. Dercle, S. Champiat, S.R. Han, L. Verlingue, D. Brandao, A. Lancia, S. Ammari, A. Hollebecque, J.Y. Scoazec, A. Marabelle, C. Massard, J.C. Soria, C. Robert, N. Paragios, E. Deutsch, C. Ferte, A radiomics approach to assess tumour-infiltrating CD8 cells and response to anti-PD-1 or anti-PD-L1 immunotherapy: an imaging biomarker, retrospective multicohort study, Lancet Oncol. 19 (2018) 1180–1191.

[121] R.R. Colen, T. Fujii, M.A. Bilen, A. Kotrotsou, S. Abrol, K.R. Hess, J. Hajjar, M.E. Suarez-Almazor, A. Alshawa, D.S. Hong, D. Giniebra-Camejo, B. Stephen, V. Subbiah, A. Sheshadri, T. Mendoza, S. Fu, P. Sharma, F. Meric-Bernstam, A. Naing, Radiomics to predict immunotherapy-induced pneumonitis: proof of concept, Investig. New Drugs 36 (2018) 601–607.